Reports and Technical Reports | All Technical Reports Collection

1985-06

# The East Greenland Polar Front in autumn

## Paquette, Robert G.; Bourke, Robert H.; Newton, John L.; Perdue, William F.

http://hdl.handle.net/10945/29257

NPS-68-85-021

# NAVAL POSTGRADUATE SCHOOL
## Monterey, California

THE EAST GREENLAND POLAR FRONT IN AUTUMN

by

Robert G. Paquette, Robert H. Bourke,
John L. Newton, and William F. Perdue

June 1985

Approved for public release; distribution unlimited

Prepared for:
Director, Arctic Submarine Laboratory
Naval Ocean Systems Center
San Diego, CA 92152

NAVAL POSTGRADUATE SCHOOL
Monterey, California 93943


Rear Admiral R. H. Shumaker                David A. Schrady
Superintendent                             Provost

This report was prepared by:

| REPORT DOCUMENTATION PAGE | | READ INSTRUCTIONS BEFORE COMPLETING FORM |
|---|---|---|
| 1. REPORT NUMBER<br>NPS 68-85-021 | 2. GOVT ACCESSION NO. | 3. RECIPIENT'S CATALOG NUMBER |
| 4. TITLE *(and Subtitle)*<br><br>The East Greenland Polar Front in Autumn | | 5. TYPE OF REPORT & PERIOD COVERED<br>Final<br>1 Aug 1984–1 Jun 1985 |
| | | 6. PERFORMING ORG. REPORT NUMBER<br>NPS 68-85-021 |
| 7. AUTHOR(s)<br>Robert G. Paquette, Robert H. Bourke,<br>John L. Newton, and William F. Perdue | | 8. CONTRACT OR GRANT NUMBER(s)<br><br>N 66001-84-WR 00376 |
| 9. PERFORMING ORGANIZATION NAME AND ADDRESS<br>Naval Postgraduate School<br>Monterey, CA 93943 | | 10. PROGRAM ELEMENT, PROJECT, TASK AREA & WORK UNIT NUMBERS<br><br>Element: 63522N |
| 11. CONTROLLING OFFICE NAME AND ADDRESS<br>Arctic Submarine Laboratory<br>Code 54, Bldg. 371, Naval Ocean Systems Center<br>San Diego, CA 92152 | | 12. REPORT DATE<br>Jun 1985 |
| | | 13. NUMBER OF PAGES<br>7 |
| 14. MONITORING AGENCY NAME & ADDRESS*(if different from Controlling Office)* | | 15. SECURITY CLASS. *(of this report)*<br><br>Unclassified |
| | | 15a. DECLASSIFICATION/DOWNGRADING SCHEDULE |

16. DISTRIBUTION STATEMENT *(of this Report)*

Approved for public release; distribution unlimited

17. DISTRIBUTION STATEMENT *(of the abstract entered in Block 20, if different from Report)*

18. SUPPLEMENTARY NOTES

19. KEY WORDS *(Continue on reverse side if necessary and identify by block number)*

East Greenland Current          Marginal Ice Zone
East Greenland Polar Front      Molloy Deep Eddy
Fine structure                  Greenland Sea
NORTHWIND                       Double-Diffusion

20. ABSTRACT *(Continue on reverse side if necessary and identify by block number)*

Closely spaced salinity and temperature measurements in the region of the East Greenland Polar Front from 75°N to 79°N in October-November 1981 are presented. The Return Atlantic Current (RAC), having a core of relatively warm and saline Atlantic Intermediate Water (AIW) (T = 0.5° to 3.0°C, S = 34.0 to 35.0), was found everywhere along a steep front separating it from the colder, fresher Polar Water. A narrow frontal jet was found to have velocities greater than 0.80 m/s where the station density was great enough to

resolve its concentrated character.  Notable fine structure was present, especially in the warm AIW just east of the front.  A cold, saline water, forming a knee in the temperature-salinity correlation, was present in the upper margins of the RAC.  The knee is formed primarily by warm AIW or Atlantic water flowing under the upper layers of water flowing from the Arctic Ocean.  Calculations are presented to show that an initially isothermal underflow could be modified to a thick thermocline by double diffusion. Calculations of the rate of cooling of fine-structure elements by double diffusion indicate that the fine structure would have a limited lifetime (about 12 days) if its waters were not continually replenished.

# The East Greenland Polar Front in Autumn

Robert G. Paquette, Robert H. Bourke, John F. Newton,[1] and William F. Perdue[2]

Naval Postgraduate School, Monterey, California

Closely spaced salinity and temperature measurements in the region of the East Greenland Polar Front from 75°N to 79°N in October-November 1981 are presented. The Return Atlantic Current (RAC), having a core of relatively warm and saline Atlantic Intermediate Water (AIW) ($T = 0.5°$ to $3.0°C$, $S = 34.9$ to $35.0$), was found everywhere along a steep front separating it from the colder, fresher Polar Water. A narrow frontal jet was found to have velocities greater than 0.80 m/s where the station density was great enough to resolve its concentrated character. Notable fine structure was present, especially in the warm AIW just east of the front. A cold, saline water, forming a knee in the temperature-salinity correlation, was present primarily in the upper margins of the RAC. The knee is formed primarily by warm AIW or Atlantic water flowing under the upper layers of water flowing from the Arctic Ocean. Calculations are presented to show that an initially isothermal underflow could be modified to a thick thermocline by double diffusion. Calculations of the rate of cooling of fine-structure elements by double diffusion indicate that the fine structure would have a limited lifetime (about 12 days) if its waters were not continually replenished.

## Introduction

A marked temperature front, seen also in the salinity and density, exists along the boundary between the Polar Water (PW), flowing southward as part of the East Greenland Current (EGC) along the Greenland coast, and the Atlantic Intermediate Water (AIW) and Atlantic water (AW) present toward the east (see Figure 1). These water masses will be precisely defined later in this section. We shall call this front the East Greenland Polar Front (EGPF), after *Wadhams et al.* [1979], as a name more descriptive than the older "Polar Front." In summer the front extends generally from the southern tip of Greenland to latitudes greater than 80°N and may be seen approximately in this length in the diagrams of *Dietrich* [1969] that are based on the cruises during the International Geophysical Year of 1958.

The present paper is concerned with the portion of the front north of 74°N and will present the results of a cruise by USCGC *Northwind* to the marginal sea ice zone (MIZ) of the EGC in October-November 1981 wherein most of the measurements are within the ice-covered portion of the East Greenland Current. A preliminary analysis of the cruise data, concentrating mainly on the frontal characteristics as interpreted from several transects across the EGPF, was conducted by *Perdue* [1982]. These and the results of Westwind 1979 [*Newton and Piper*, 1981] in August-September 1979 are the only measurements from the frontal zone with relatively high resolution both in the vertical and horizontal. They are based on modern conductivity-temperature-depth (CTD) recorders and on station spacings as small as 5–30 km. The MIZEX expedition operated in the northern part of this area in summer 1983, but its results are not yet available.

The Nansen bottle data that are close to or cross the front above 74°N and thus are suitable for comparison are the August-September 1962 data of *Atka* [*Gladfelter*, 1964], which barely cross the front; Edisto 1964 [*Codispoti*, 1968]; and Edisto 1965 (unpublished data, 1965). Some information about the effects of autumn are obtainable from the cruises of *Aisberg* in late October 1959 near 74°30′N and *Polyarnik* in the same area in early October 1958. Two stations from *Polyarnik* in mid-October 1963 on 78°N reach west only to 1°E and are useful mainly for estimating autumn temperatures east of the front at that latitude.

During the discussion of previous knowledge about the northern Greenland Sea, reference again will be made to Figure 1, which is a composite of representations of the circulation of the North Atlantic Ocean that is derived from several sources and somewhat simplified. From *Dietrich* [1969] and *Kiilerich* [1945] is derived the general form of the circulation in the EGC, the Norwegian Current, and the West Spitzbergen Current (WSC); Kiilerich shows considerable detail in the Greenland shelf area and particularly the turning westward of the EGC near 76°N. The westward turning vectors north of 76°N are derived from the present work. From *Gladfelter* [1964] are derived the forms of the recirculation paths for water turning southward from the north-going WSC into the EGC. Considerable definition is added to the location of the EGPF and the frontal jet by the present work and, farther north, by the work of *Newton and Piper* [1981]. The extension of the jet to the south of 74°N is inferred from Dietrich's maps but also can be verified in three crossings, reaching south to 70°30′N, from the data of Edisto 1965 (unpublished data, 1965) as well as other cruises. It is interesting that the front and the jet follow the continental slope closely as far north as 77°N. From this latitude northward the front veers away toward the east into deeper water.

Some of the features of the frontal zone that will be elaborated here have been known in less detailed form for many years. *Aagaard and Coachman* [1968a] outlined the early history of investigations in the Greenland Sea; a summary of pertinent aspects of their discussion follows. The existence of the EGC and the associated ice stream was known well before the turn of the century. That there was a front along the eastern side of the EGC was known, but there was little emphasis upon it at those times. It was presumed that the warm, saline water to the east of the ice must originate in the Atlantic Water (AW) of the West Spitzbergen Current. The existence of a more rapid flow of ice southward near the eastern boundary of the EGC also was known. During the early part of the present century, more became known about the circu-

Fig. 1. Bathymetry and currents in the Greenland-Norwegian Sea derived from a variety of sources (see text). Depth labels are in hundreds of meters. The 5600-m depression on 79 N, called the Molloy Deep, is a possible cause of a persistent eddy. The Greenland to Spitzbergen strait is now being called Fram Strait.

lation of the Greenland Sea and the warm AIW concentrated along the eastern side of the front. The latter was seen as arising in a reversal of the flow of part of the north-going WSC occurring between 75°N and an undefined latitude north of 80°N. For this flow the term "Return Atlantic Current" has gained some acceptance [see *Jakhelln*, 1936; *Gladfelter*, 1964; *Codispoti*, 1968].

In the present work the Return Atlantic Current (RAC) is found to be a notable feature and requires more emphasis than that given in previous work. The current gains its identity from being a core of warm, high-salinity water, often broken into differing filaments, most of it being above 0°C and near the high end of the salinity range for AIW, even overlapping into AW. Property limits for these waters are described later in this paper. The RAC has a width of 100 km or less and lies along the EGPF at depths roughly between 50 and 300 m, commonly at least partly under the PW. The reader may wish to look ahead to Figures 4, 5, 6, and 7 for illustration. Its center has a temperature maximum both in the vertical and east-west directions. The temperature maximum in the vertical disappears toward the east; toward the west the maximum

decreases in temperature and, before it disappears, is found at the bottom, well up on the shelf. The center has a salinity maximum in the vertical, usually coincident with the temperature maximum, or nearly so. Toward the west, the salinity decreases. Toward the east, the change in the salinity at the maximum is small, and it is presently not obvious whether it increases or decreases.

*Aagaard and Coachman* [1968a] deduced that the flow of the EGC in winter approximated $35 \times 10^6$ m$^3$/s. Most of this would have to be AIW because, according to *Aagaard and Greisman* [1975], the outflow of PW from the Arctic Ocean approximates $1.8 \times 10^6$ m$^3$/s. In our view all or nearly all of the AIW associated with the EGC is RAC; hence this large transport was chiefly due to the RAC. Aagaard and Coachman deduced their large transport from current measurements made from the ice island Arlis II as it drifted during the late winter from 77°45'N, 9°36'W on the East Greenland shelf to 69°N, 20°25'W in 1400 m of water, now well down the continental slope. They construed this diagonal drift as equivalent to a transverse section normal to the current for purposes of transport calculation. The applicability of these results to con-

ditions in autumn is questionable because Aagaard and Coachman present limited evidence that the transport decreases by a factor of perhaps 10 in summer.

More recent direct measurements of current have been made by *Vinje* [1977a, 1978, 1979] using satellite-tracked large ice floes and ice-mounted buoys. These will be discussed later.

The warm water on the eastern side of the EGPF is appropriately called AIW after *Aagaard and Coachman* [1968a], who put the lower salinity and temperature limits for this water at about 34 and 0°C, respectively. By implication their upper limits for salinity and temperature were set at the lower limits for AW, i.e., salinity 35.0 and temperature 3°C. They described colder and more dilute water as PW and further suggested that AIW is formed by mixing PW with AW. However, as will be seen later, additional cooling sometimes must be involved. AW was defined by *Swift and Aagaard* [1981] and *Carmack and Aagaard* [1973] as having a temperature greater than 3.0°C and a salinity greater than 34.9, a relaxation of the salinity limit from the traditional 35.0. Swift and Aagaard defined an upper and a lower Arctic Intermediate Water (UAIW and LAIW), the lower division corresponding to the more recent definitions of Atlantic Intermediate Water above. Their UAIW is a warm (>2°C) water with a salinity of 34.7–34.9. This UAIW is associated with a temperature minimum that exists when warmer, slightly diluted AW overlies LAIW. Their temperature minimum does not exist in most of our data because our surficial wters are nearly all cold. In our data, water having the characteristics of their UAIW is so closely associated with water they could call LAIW that it is more appropriate to adhere to the older Carmack and Aagard definition of Atlantic Intermediate Water that included both UAIW and LAIW.

For the sake of completeness, Greenland Sea Deep Water (GSDW) is defined. This water lies beneath the AIW, deeper than about 800 m, and only its upper fringe appears in our cross sections. It was described by *Carmack and Aagaard* [1973] to have $T < 0°C$ and $34.85 < S < 34.95$. *Swift and Aagaard* [1981] subdivide this water into Greenland Sea Deep Water and Norwegian Sea Deep water, a distinction that can serve no purpose in the present paper.

In the past an arbitrary boundary for the EGC has been set for purposes of water classification. *Aagaard and Coachman* [1968b, p. 269] specify the 0°C isotherm or the 34.5 isohaline at 50 m depth. Presumably, whichever determinant is the farther east controls. *Gladfelter* [1964] used the 0°C isotherm at any depth to 75 m. In Gladfelter's data these boundaries coincide fairly well with the most easterly isopleth of dynamic height, implying continued southward flow. However, it will be seen later that southerly flow existed in at least one data set to the east of these limits along 78°N.

The present paper will concentrate on the aspects of the data that are relatively new:

a description of the front based on a high-resolution measurements in autumn; a comparison with summer historical data.

a demonstration of remarkably high baroclinic speeds in a jet near the ice margin; an indication that such a jet exists to latitudes as far north as 81°30'N; a notable on-shelf component of velocity near 77°N.

a description of fine structure in both the AIW and PW and some conclusions regarding size of the elements and the dissipation time. This will lead to a conclusion that the heat in the AIW under the PW is maintained by continual westward advection of AIW. Some of the fine-structure elements will be shown to have surprisingly large compensating swings in temperature and salinity while the density increases only slightly with depth.

a demonstration that AIW, overlaid by PW, contains an intervening water type colder than can be obtained by linear mixing between AW and PW. This water can be formed by double diffusion, it may be a remnant of winter freezing effects or it may advect from the north.

## METHODS

The measurements were made with a Neil Brown Instrument Systems Mark III conductivity-temperature-depth recorder interfaced with a Hewlett-Packard 9835B desk-top computer sampling three times per second, approximately three times per meter of depth. The sensor cage of the instrument was shrouded in 1.25-cm mesh (0.5-in) hardware cloth to protect the sensors from the ice slush prevalent alongside the ship. This shroud undoubtedly affected fine-structure measurements to a minor extent but probably at length and temperature scales smaller than those with which we are concerned.

Prior to lowering the instrument it was flushed by hoisting and lowering over a depth range of 100 m for several minutes to minimize temperature errors caused by stored heat in the body of the instrument. At about half of the stations, recordings were made both during lowering and hoisting in order to detect anomalies. No important anomalies were found. Standardization of the instrument was by means of a reversing bottle clamped to the line above the instrument. The resulting samples were analyzed by a deck salinometer referenced to standard water. The average differences between the instrument and the standards were approximately 0.01°C in temperature and 0.01 in salinity, not notably greater than the probable error in the thermometers and the deck salinometer measurements. Hence no correction was applied.

There was minor salinity spiking, which is unimportant for all purposes except the close inspection of the salinity-temperature-density relation near station 95. To date, only these latter stations were despiked, using standard techniques.

## DESCRIPTION OF THE FRONT AND CONTIGUOUS WATERS

The water properties in Northwind 1981 are presented in the form of six vertical cross sections (Figures 3–8) crossing the front along the lines shown in Figure 2. Details pertinent to each crossing are listed in Table 1. The most northerly crossing (crossing 6 in Figure 3) did not succeed in crossing onto the shelf and appears only to have touched the eastern edge of the warmer filaments of flow along the front; these filaments can be seen in their entirety in the more southerly crossings. Station 79 is close to being in the edge of the WSC. The warm AW here is submerged beneath overlying PW and ice above to depths greater than 100 m. The salinity of much of this water is greater than 34.9 and, in fact, exceeds 35.0 in the center of the core at 200 m. Hence it can be classed as AW by the *Swift and Aagaard* [1981] definition. Since station 79 is so close to the WSC, it is reasonable for AW coming from that source to be only slightly modified.

The peaking of isotherms near station 81 suggests a cyclonic eddy, since it mirrors the density structure. A similar eddy observable in historical data in the same location will be illustrated under "Historical Comparisons."

The well-defined RAC may be seen in Figures 4 and 5, transects along 78°N. In Figure 4 the earlier of the two sections, the warm core, close against the PW and under PW and ice is seen to have the characteristics of AW at its center, diluting and cooling to AIW above and, more slowly, toward
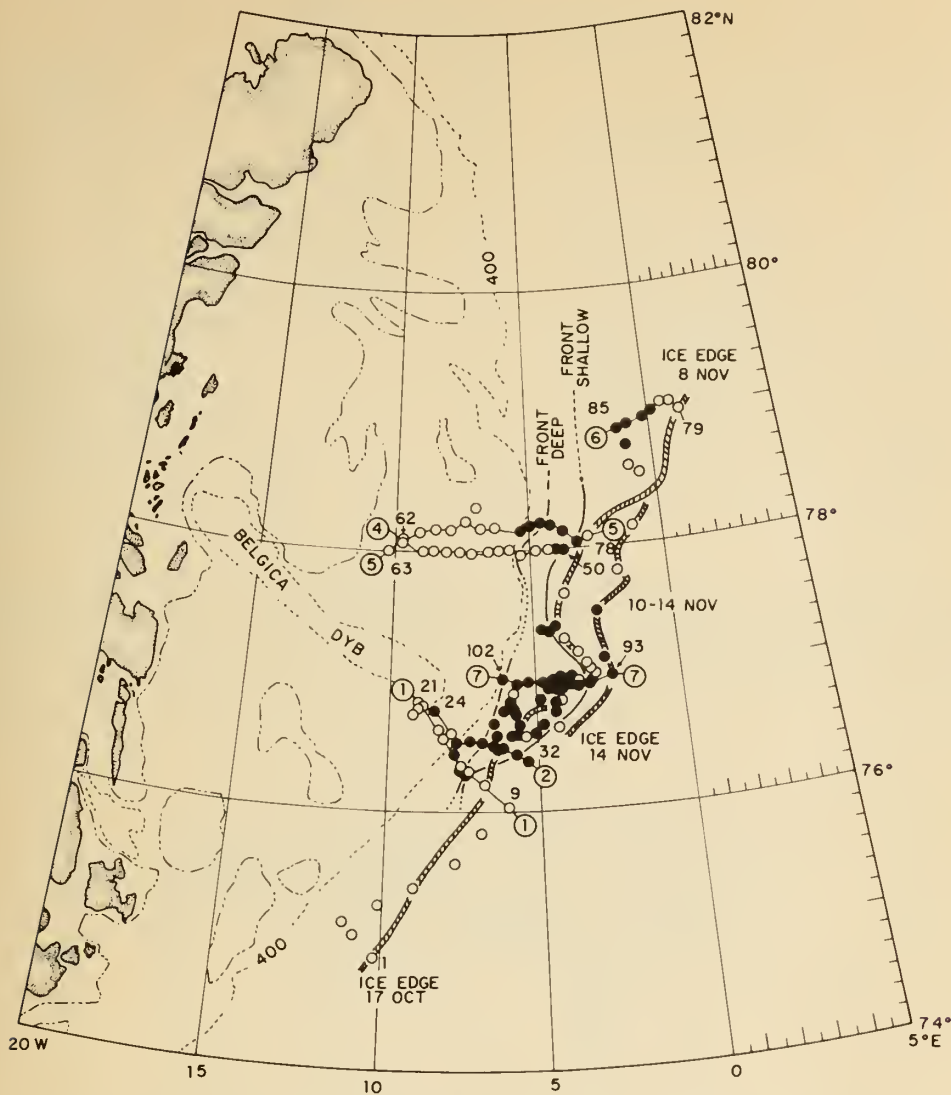
Fig. 2. Station positions for Northwind 1981. The 400-m isobath is dashed; the 200-m isobath is shown with an interrupted dash. Filled black dots show stations with fine-structure excursions greater than 0.1°C. Frontal crossings referenced in the text are labeled with numbers in circles. Station numbers are in italics. The shallow manifestation of the front is approximately at the point of extrapolation of the frontal isohalines to the surface; the deep end is the point where isohalines suddenly become markedly less steep at 200–350 m.

the properties of GSDW beneath. In Figure 5 the core becomes filamental in structure, and its maximum temperature drops below 3°C, the temperature limit set by *Swift and Aagaard* [1981] for AW, and it may appropriately be called AIW.

It will be noted in Figure 4 that the warm core of AIW east of the front is separated by a distinct temperature gradient not only from the PW but also from a warm water layer that underlies the PW and extends well back onto the continental shelf. A similar statement may be made with regard to Figures 5–8, except that in these figures the core is not centralized but is more or less broken down into filaments. This suggests that the warm AIW core east of the front has a tendency to retain its identity, even to depths of 300 m or more, as it progresses southward with the RAC. The layer of water warmer than 0°C on the shoreward side of the front is a cooler, slightly fresher variant of the AIW found far back on the Greenland Shelf in summer by *Newton and Piper* [1981].

The second crossing on 78°N (Figure 5) was an eastward traverse over essentially the same line as the first. The center

of the warm core at station 74 was sampled on November 7, 10 days later than the corresponding station 52. Now the warm core is somewhat cooler, and it has broken up into a complex fine structure consisting of filaments or lenses of AIW of contrasting temperatures. This complexity is more common than are the relatively undisturbed warm cores like the one in Figure 4. The maxima and minima of those lenses occur over a narrow density range, and the water column remains stable, as will be illustrated during the examination of station 95 later in this discussion.

In many of the crossings that extended onto the shelf there is, on the western side of the front at depths of 150 to 300 m, an isolated parcel (or parcels) of AIW; one of these may be seen centered near station 73 in Figure 5. Other instances of this phenomenon were seen in the crossings of *Northwind* in 1979 [*Newton and Piper*, 1981].

The two southerly crossings extending to the sill at the entrance to Belgica Dyb (Figures 6 and 7) are not greatly different in character from those just discussed. As later quantitative calculations will show, one would expect a moderate

TABLE 1.   Ice Margin Transect Data

| Transects | Stations | Dates | Duration, hours | Ice Edge Position | Approximate Latitude |
|-----------|----------|-------|-----------------|-------------------|----------------------|
| 1 | 9–21 | October 18–21 | 64 | XBT station 23 | NW, 76–76.8°N |
| 2 | 24–32 | October 24–25 | 24 | Between stations 29 and 30 | 76.5°N |
| 4 | 50–62 | October 28–30 | 39 | 2 km west of station 50 | 78°N |
| 5 | 63–78 | November 3–8 | 132 | Between stations 77 and 78 | 78°N |
| 6 | 79–85 | November 8–10 | 26 | 2 km west of station 79 | 79°N |
| 7 | 93–102 | November 11–12 | 29 | 1.5 km west of station 93 | 77°N |
| ED 64 | 9–12, 45–49 | September 2–13 | 272 | | 79°N |
| ED 65 | 21–29 | August 31 to September 2 | 50 | | NW, near 75°N |
| ED 65 | 30–39 | September 5–7 | 50 | | 78.3°N |
| ED 65 | 43–47 | September 11–12 | 14 | | SE, 77°–76°N |
| AK 62 | 27, 26, 38 | August 19–25 | 124 | | 78°N |

Numerals refer to Northwind 1981, ED to Edisto, AK to Atka.

decrease in temperature of the warm core by double diffusion during flow of the core southward. However, the observed decrease is no larger than the temporal change already observed in a few days on the two northerly crossings. Further, a temporal bias exists in that water at more southerly latitudes along the front left the northerly regions at a warmer season. Hence decreases in temperature that might have occurred otherwise tend to be obscured.

The most notable feature of Figure 6, which is the more southerly crossing, is the presence well up on the shelf of an
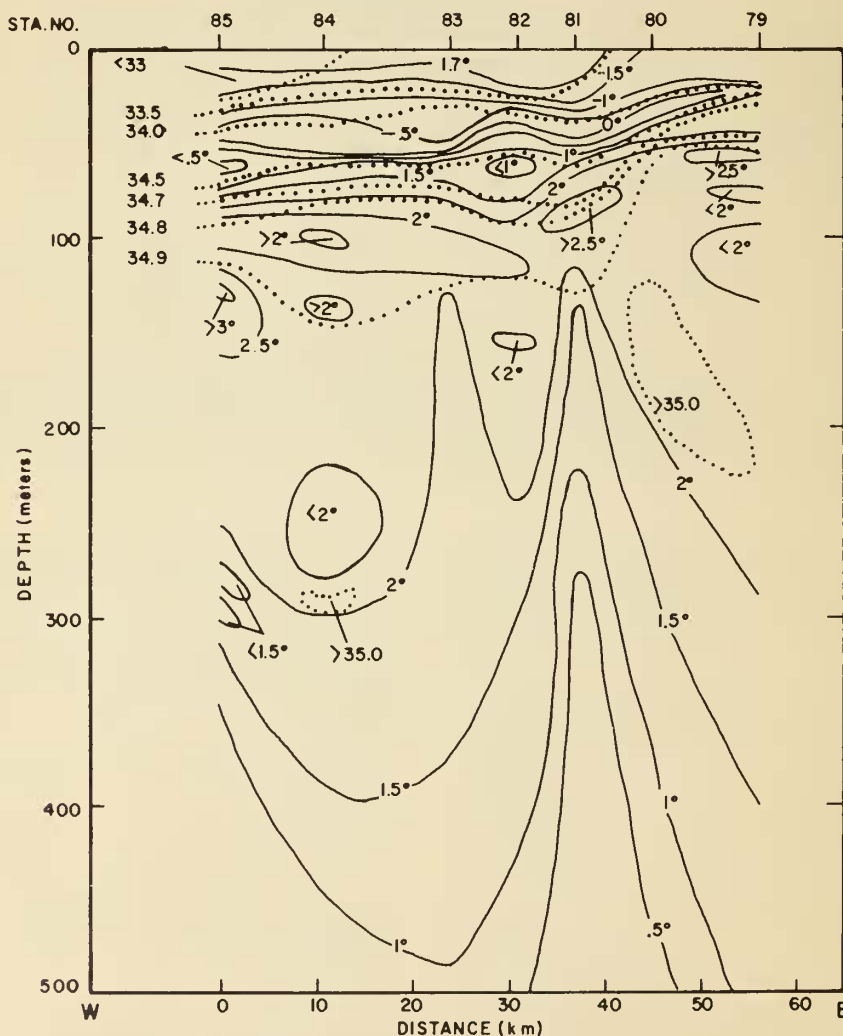


Fig. 3.  Transect 6 on about 79 N. The warmest part of the Return Atlantic Current is just visible on the left. The peaking of isotherms near station 81 corresponds to a cyclonic eddy found also in other data. In this figure and in all other transects the temperatures are shown as solid lines and the ice salinities as dotted Lines.
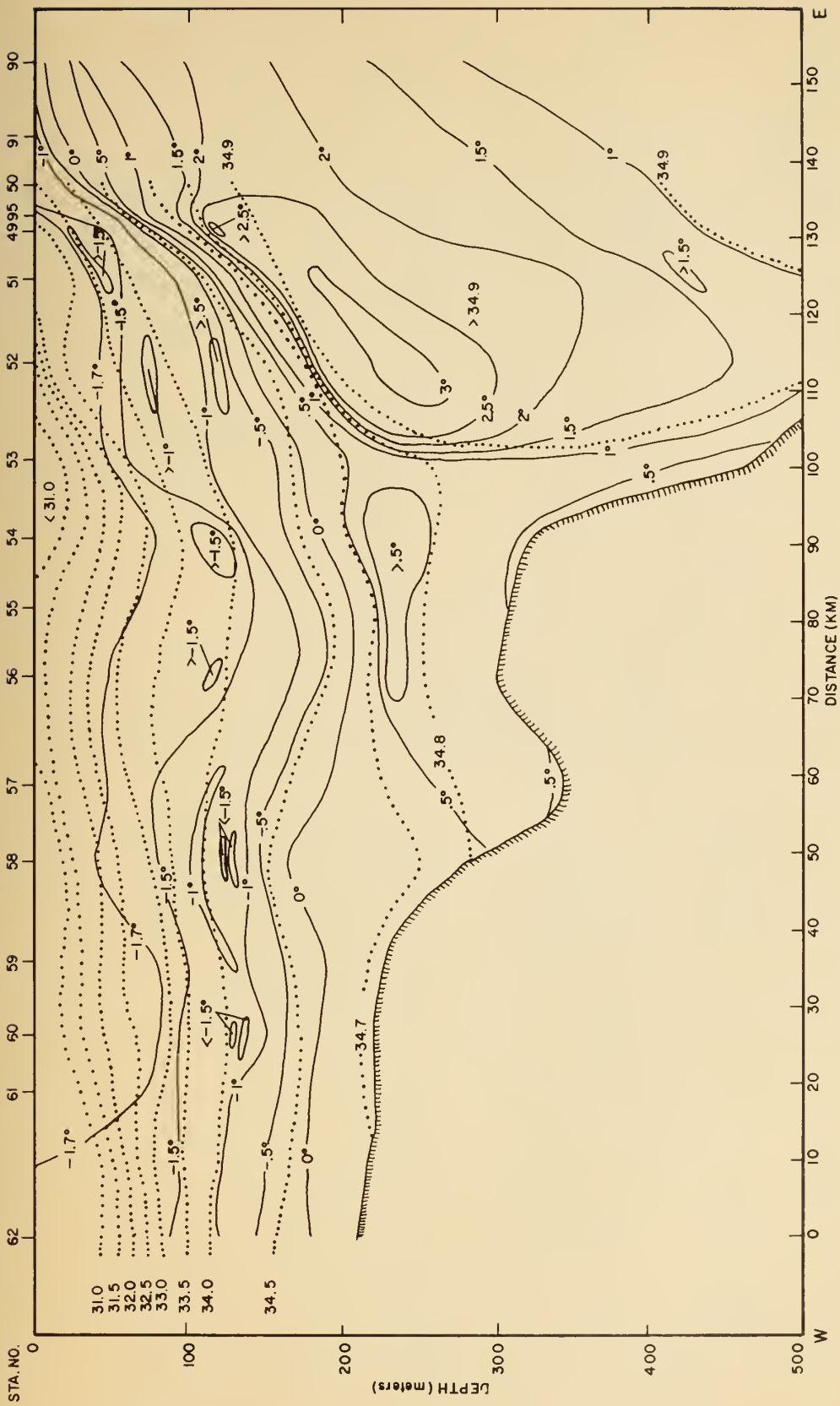
Fig. 4. Transect 4 on 78°N. Stations 90, 91, and 95 are XBT drops. This section shows the warmest, most saline core of Return Atlantic Current and is the only sectioning of the core relatively free of major fine structure.
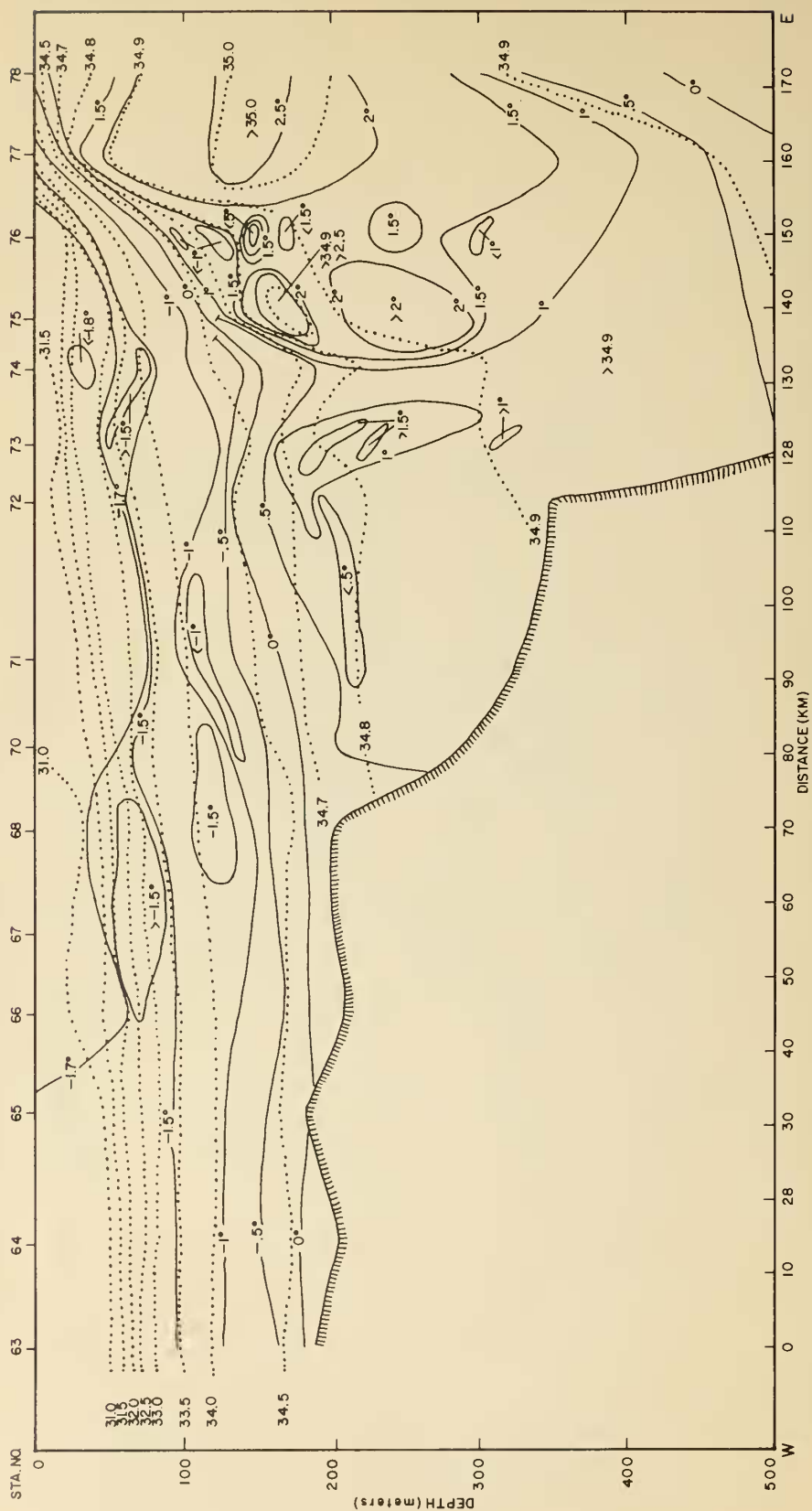
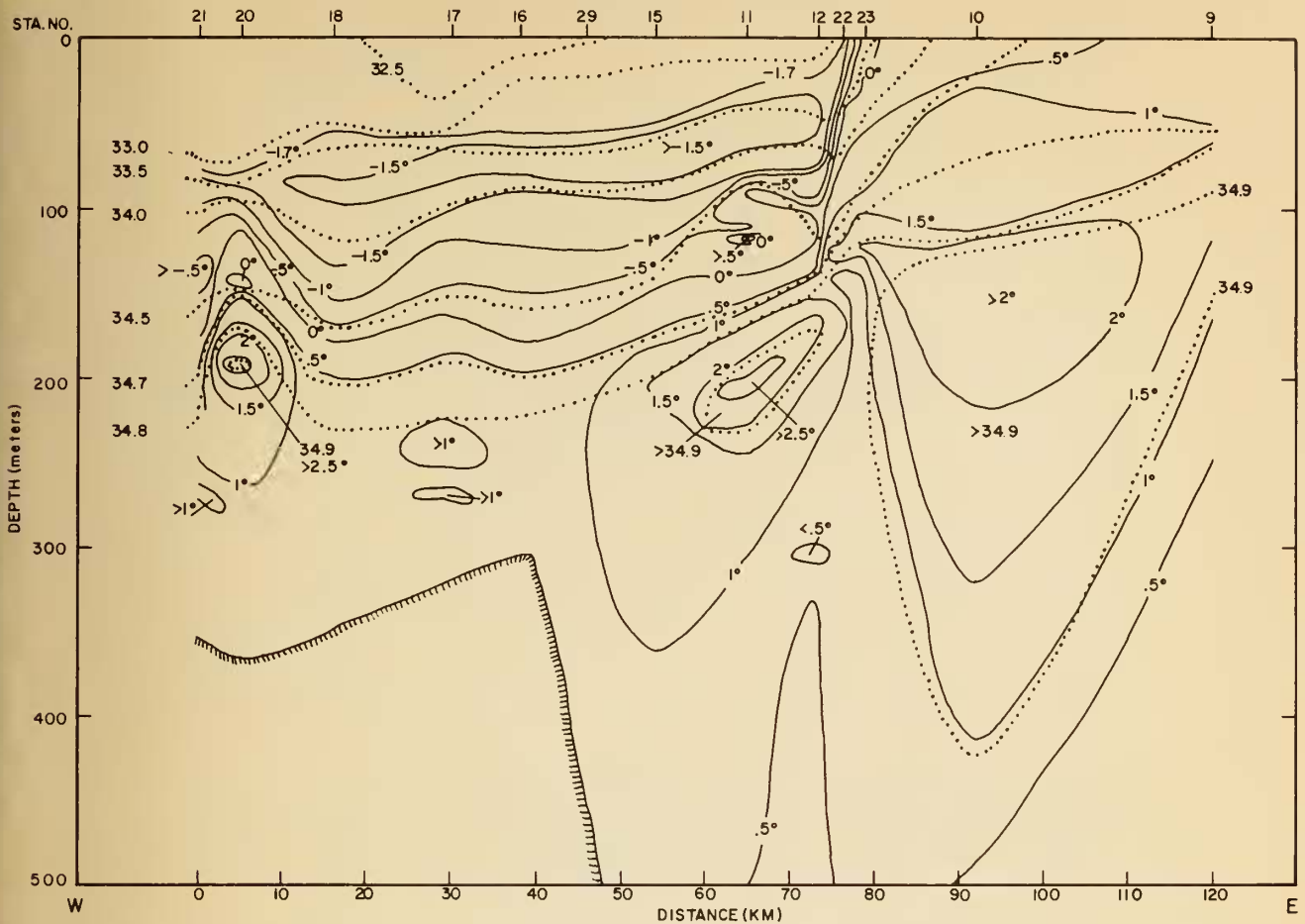Fig. 5. Transect 5 on 78°N. In the five intervening days since transect 4, notable fine structure has developed.

Fig. 6. Transect 1, 76°N–76°48′N. The leftmost edge of this transect reaches the sill at the mouth of Belgica Dyb. Note the parcel of AIW close to the sill, essentially of the same properties as the warmest AIW 90 km to the east.

isolated parcel of AIW with a center as warm and nearly as saline as water 60 km and more to the east, in the region of the well-defined front. A similarly large parcel is separated from the main portion of the warm core, seemingly poised to follow a similar route. An "isentropic" path between the two parcels exists close to the 34.9 isohaline. This rather notable tendency to move parcels of warm water onto the shelf in this area probably is associated with the baroclinic circulation, which may be seen to take a sharp turn toward the coast in the dynamic topographies to be discussed in the section "Velocities and Transports."

Another notable feature is the change in the near-surface frontal slope between the two crossings. The later crossing in Figure 7 shows the surface PW having spread eastward some 30 km relative to its position 7 days earlier. This could easily happen under the influence of a westerly wind blowing the ice into warm water with resultant cooling and dilution.

A cross section from the central part of the area studied is shown in Figure 8. Here the ship did not penetrate to the 500-m depth contour, but the warm core is above bottom depths of 1100 to 2000 m, over the central part of the continental slope. Notable in this crossing is the extreme complexity of interleaving and fine structure. This has prompted an investigation to demonstrate that the density increases monotonically downward; this investigation will be presented under "Fine Structure." Stations 95 and 96 also have been made the subject of an analysis of double-diffusive rates by *Bourke et al.* [1983].

## HISTORICAL COMPARISONS

It is of interest to compare the front in autumn with conditions in summer. Five historical summer transects in the region of the present survey are mapped in Figure 9. Of these, two are reasonably coincident with 1981 transects: the northernmost line, from Edisto 1964, and stations 30–39 from Edisto 1965. The other two from Edisto 1965, while they show no notable disagreements with the present results, are either too short or too distant from any of the present transects to be satisfying. The fifth transect, from USS *Atka* in 1962, will be used in the discussion of the transport of the EGC.

The Edisto 1965 data are to be compared with Figures 4 and 5; they are shown in Figure 10 with the positions of the corresponding stations of Figure 5 marked. Even though there is less ice in summer, as can be seen from the above-freezing surface temperatures, the edge of the PW is approximately in the same location summer and fall, i.e., over the continental slope. A lobe of AIW extends downward and westward beneath the PW in the Edisto data. This corresponds to the RAC in the present results, but the maximum temperature of the lobe is only 1.6°C near the 235-km graduation. However, it should be noted that higher temperatures might have been found if the measurements had been carried out with closer station spacings. The distribution of isohalines is remarkably similar to that of autumn 1981.

The highest temperatures in the Edisto 1965 section are all present near surface and at the most easterly station, which is
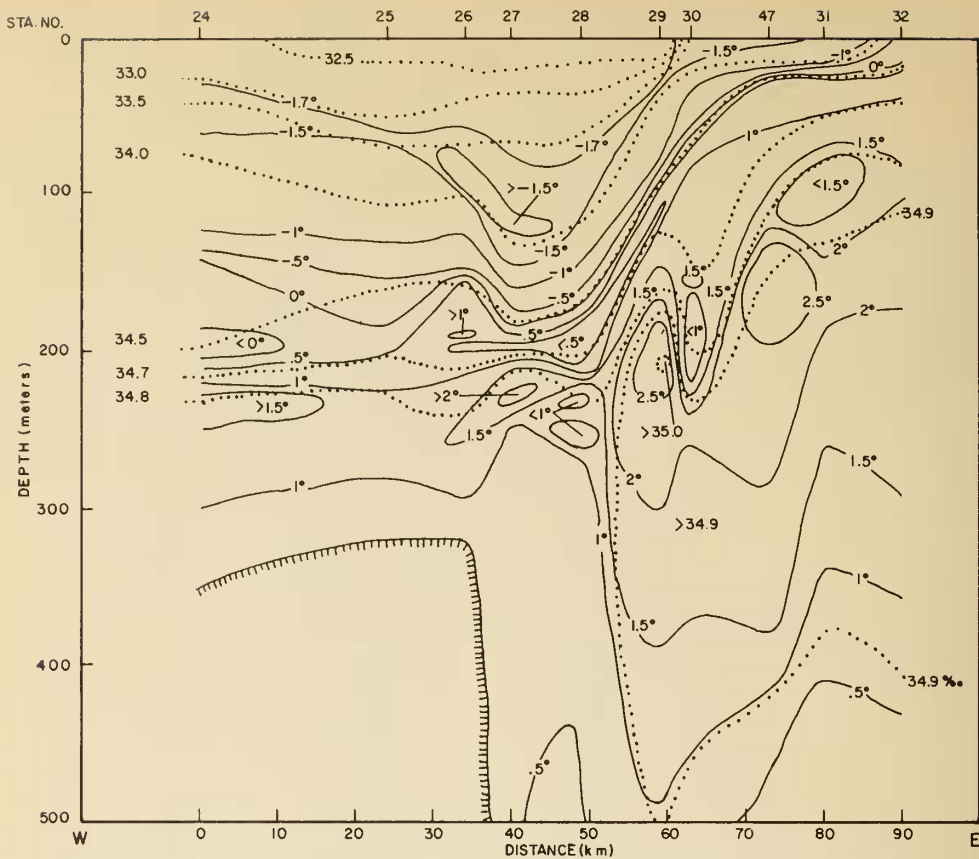
Fig. 7.  Transect 2 on about 76°30′N. Little degeneration in temperature and salinity of the warm core is to be seen as compared to transect 4, 280 km to the north.

45 km east of the end of our line. The high temperatures are associated with salinities between 33.0 and 34.8, generally less saline than in the warm under-ice core in the present data.

The Edisto 1964 section is presented similarly in Figure 11 and is to be compared with Figure 3. The Northwind 1981 data are just to the east of the frontal slope and seem to have touched the core of the RAC on the west, judging from the presence of the 3°C isotherm. Except for the not surprising covering of the surface by ice in 1981, the two sections correspond well. Most interesting is the peaking of isohalines at the 280-km point in 1964 (which also corresponds to a peaking of isopycnals), occurring in the same location as the peaking of isotherms in 1981. Both correspond to cyclonic eddies. The eddy at the 350-km mark was pointed out in this data set by *Aagaard and Coachman* [1968b], who suggested general causes for it. An eddy in this general location also was noted in satellite imagery of the ice margin by *Vinje* [1977b] and by *Wadhams and Squire* [1983]. The latter authors noted a possible correlation with the nearby Molloy Deep, the 5570-m depression to be seen near 79°N in Figure 1. However, they favored baroclinic instability as the generating mechanism. Recently, *Smith et al.* [1984] proposed that the eddy is topographically generated by the Molloy Deep, supporting their conclusion with a numerical model. Interestingly, the westernmost eddy in 1964 is not the classical cold-core type because, in this case, salinity is more important than temperature in controlling the density.

In its external characteristics the EGPF in *Northwind* 1981 has a slope in its steeper parts varying from 4 to 14 m/km when measured by isohalines and from 4 to 21 m/km when measured by isotherms. These numbers are similar to the slope of the western face of the Gulf Stream north of Cape Hatteras. In the historical early September data of Figure 10–11 the slopes of isohalines also are comparable to those in 1981. However, in September the isotherms near the surface were vertical and even reversed slope. The figures show that there is a body of warm dilute water next to the PW near surface that is of uncertain origin and causes this difference between isotherm and isohaline slopes.

## VELOCITIES AND TRANSPORTS

Previous information about water speeds in the EGC come from a variety of sources, most of them representing summer data. Nearly all indicate that the EGC increases in velocity near the eastern edge of the ice. *Kiilerich* [1945], on the basis of a composite of hydrographic measurements between 75°N and 80°N, found a narrow jet with surface speeds up to 0.3 m/s. Farther to the west the speeds were considerably slower.

Baroclinic velocity vectors derived from Edisto 1964 and 1965 data are shown by *Aagaard and Coachman* [1968b] to have the highest speeds in the region between the EGPF and just west of the 1000-m isobath. The highest speed computed was 0.23 m/s near 77°N, 7°W. To the west of the high-speed region the speeds decreased to 0.08–0.10 m/s, with some small values in between. The shallow reference level of 200 dbar (necessitated by the shallow water) leaves open the possibility that the speeds could be substantially higher. For example, Edisto 1964 [*Codispoti*, 1968] shows the highest surface speeds at 79°N, 2°W, just seaward of the shelf but not in the high-speed core, to be approximately twice as great when the
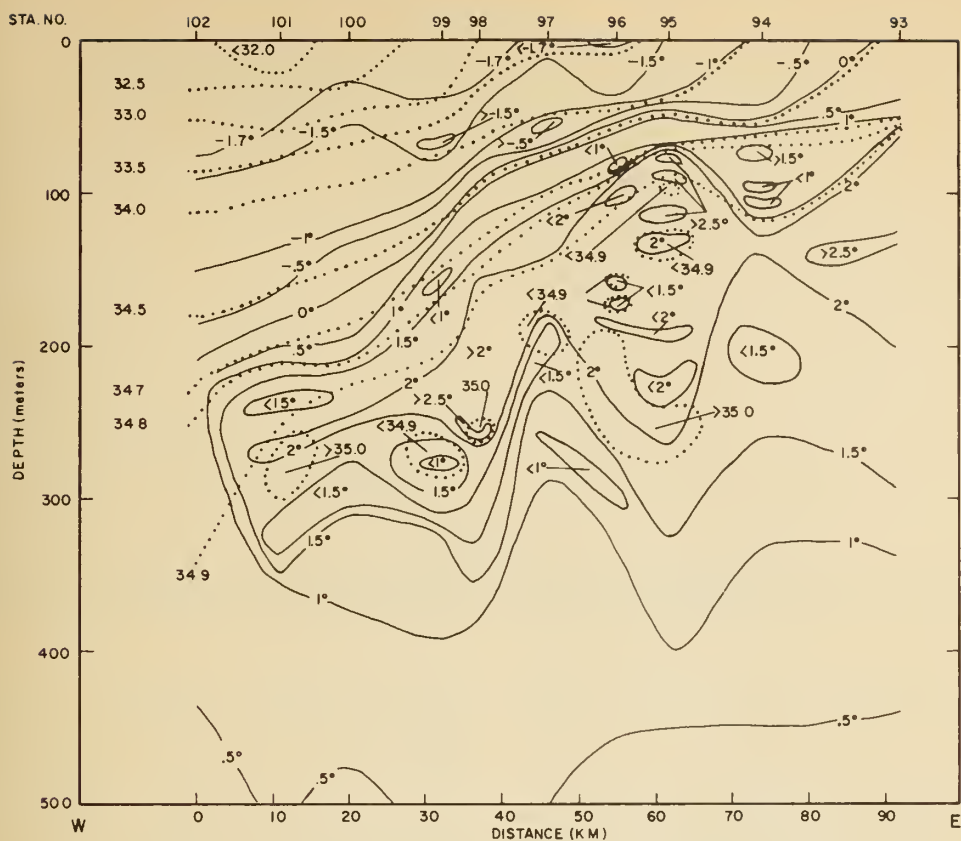
Fig. 8. Transect 7 on 77°N. Contains the most notable fine structure found during the cruise.

1000-dbar reference surface rather than the 200-dbar surface is used.

Quasi-Lagrangian measurements of velocity include the barotropic component of flow but suffer from time and space averaging so that localized high velocities seldom are revealed. Some such measurements are summarized below. In September 1965, *Edisto* was located just inside the ice edge near 78°N, 8°W [*Aagaard and Coachman*, 1968a] and drifted SSW with the ice at an estimated speed of 0.75 ± 0.25 m/s. Earth-referenced ice drift measurements reported by *Aagaard and Coachman* [1968a] were made from the drifting ice island Arlis II, located about 120 km west of the EGPF over the mid-shelf area near 77°N in February 1965. These indicate surface speeds of about 0.10 m/s. Nearer the frontal boundary,

but far to the south, drift speeds were found to average about 0.24 m/s.

More recently, *Vinje* [1977a, 1978, 1979], tracking buoys and large ice floes by satellite, found average southward drift speeds of about 0.15–0.20 m/s, generally between 75° and 80°N in late winter to midsummer. Those drifters close to the east Greenland coast approximated 0.10 m/s in speed. The highest reported speed [*Scientific Committee on Ocean Research*, 1979] was 0.30 m/s near the eastern edge of the ice
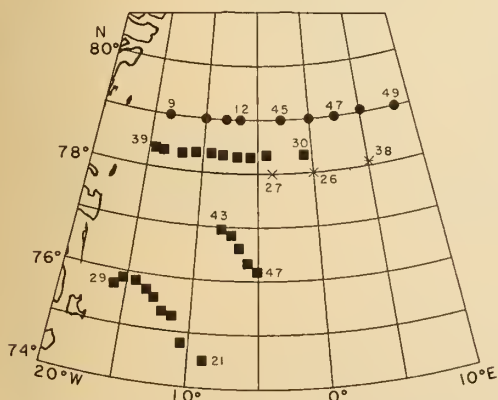


Fig. 9. Positions of historical stations referenced in the preceding figures and in the text: (asterisk) Atka 1962; (filled circle) Edisto 1964; (filled square) Edisto 1965.
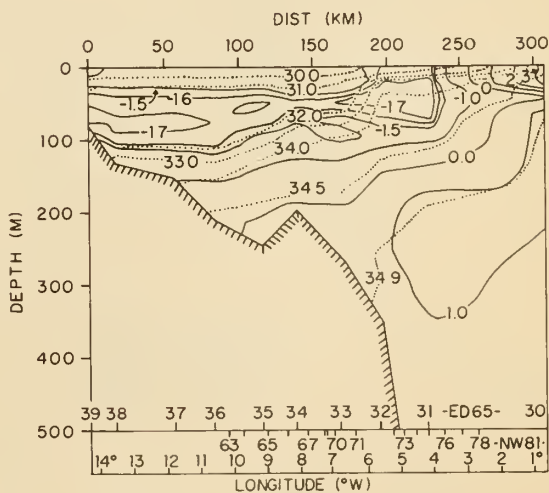


Fig. 10. Historical transect, Edisto 1965 on 78°20′N. To be compared with transects 4 and 5, Figures 4 and 5. Station positions for transect 5 and longitudes are shown. The temperatures in the warm core are colder than in autumn 1981; the temperature front extends vertically to the surface.
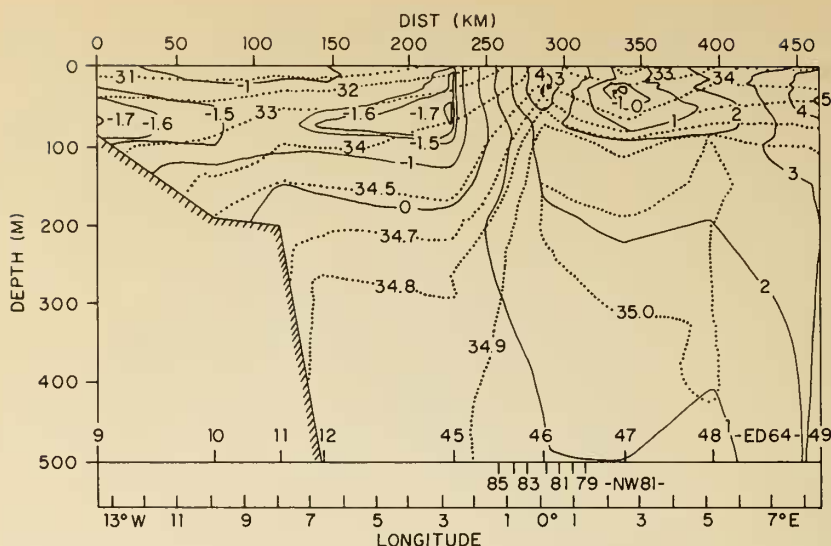
Fig. 11. Historical transect, Edisto 1964 on 79°N, to be compared with transect 6. The peaking in isotherms observed in transect 6 is echoed here in the same location by a peaking of isohalines and, in contrast, a warm core at the surface. A plot of sigma-t shows isopycnals peaking much like the isohalines, thus corresponding to a cyclonic eddy.

stream. Moderate meanderings were the rule, but there was strong wind coupling, resulting in northerly and westerly drifts at times.

The dynamic heights obtained during Northwind 1981 are shown in Figures 12 and 13, the first for the surface and the second for the 150-dbar level, both referred to 500 dbar. Where the water was shallower than 500 m the water columns beneath their greatest depths were extended to 500 dbar, using the water properties of the nearest deep-water column. This

technique is preferable to plotting the whole field of dynamic heights relative to the 200-dbar surface. Although it gives identical velocities for the extrapolated depths, the present method makes maximum utilization of the density information in deep-water columns to give more accurate dynamic heights there. Forty-one of the more westerly of the 122 stations required this approximation, i.e., they had bottom
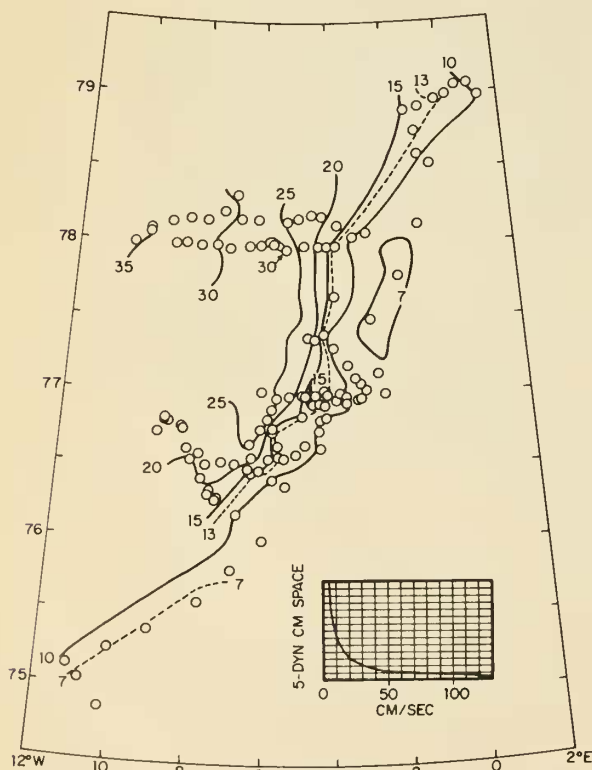


Fig. 12. Dynamic heights of the sea surface, referred to 500 dbar, in dynamic centimeters (multiply by 0.1 to obtain Joules per kilogram). The closer spacings of isopleths indicate a narrow frontal jet with baroclinic speeds exceeding 0.8 m/s.
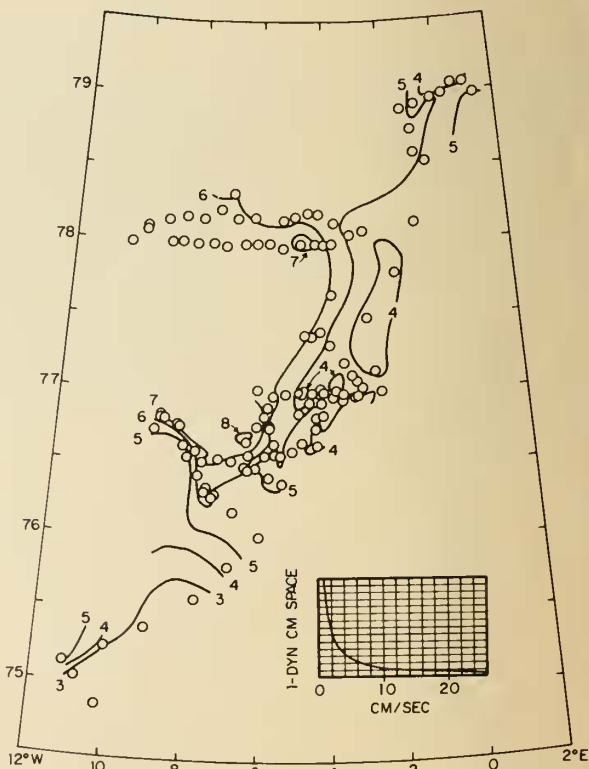


Fig. 13. Dynamic heights of the 150-dbar surface, referred to 500 dbar, in dynamic centimeters (multiply by 0.1 to obtain Joules per kilogram). Note the change to 1 dyn cm spacing of isopleths. The patterns are similar to those at the surface, except that the speeds are generally 1/3 to 1/10 as great. Near latitude 77° the westward-going isopleths indicate speeds greater than at the surface.

depths between 180 and 450 m. Fortunately, the regions of greatest velocity are over deep water and not subject to uncertainty from this procedure.

The dynamic heights at the surface agree in general with historical results. They indicate a high-speed frontal jet and velocities on the western edge of the survey area of about 0.05 m/s, about half the drift speed of Arlis II when it was a short distance to the west of the line on 78°N in winter and about half the speeds computed by earlier investigators from the few observations well up on the shelf.

One of the more striking features of the field of dynamic heights is the high speed of the frontal jet, which reaches 0.96 m/s just inside the ice edge near latitude 77°25′N and shows speeds exceeding 0.80 m/s at two locations farther south. It will be noted that the highest speeds are found when the station density is highest, which leads to the suggestion that the jet would be seen in high velocity all along the front if the station densities were high enough everywhere to resolve it. The high speeds of the jet are absent in historical dynamic topography precisely because of this lack of close station spacing, generally 2 to 3 times as great as the spacings in 1981. Some idea of the concentration of the frontal jet may be seen in the cross section of baroclinic speed components normal to the section seen in Figure 14 for the northerly line along 78°N. This section shows only moderate speeds, slightly over 0.40 m/s. There is much variability in the lower speeds to the west of the jet, probably indicative of eddy structures.

Another interesting feature in Figure 12 is the turning of isopleths westward between 76°30′N and 77°N, a phenomenon previously shown near 76°N by *Kiilerich* [1945]. Since bathymetric steering evidently guides the frontal jet, one suspects bathymetry as the cause of this general turning. Three notable bathymetric features occur near the point of turning. The east-

ern end of Belgica Dyb, a cross-shelf trough, lies at 77°N, 7°W; the ridge separating the northern and southern basins of the Greenland Sea extends southeast from the continental slope at about 77°N, 5°W at a depth of 2000–2500 m, and near the landward end of this ridge the continental slope begins to veer toward the southwest. Note that the 400-m isobath provides only a generalized outline of the break and shows only one (Belgica Dyb) of a series of cross-shelf troughs. Recently acquired bathymetric data (R. H. Bourke et al., unpublished manuscript, 1985) also shows that the indicated sill at the mouth of Belgica Dyb is minor or nonexistent; hence the sidewalls of this trough extend their influence past the shelf break. That warm water moves toward and into Belgica Dyb is indicated by two observations. *Newton and Piper* [1981] suggested this cross-shelf flow earlier, on the basis of temperatures and salinities measured along the axis of Belgica Dyb during the cruise of USCGC *Westwind* in 1979. Also, it is likely that the warm, salty parcel of AIW observed 40 km from the mouth of the trough, as seen in Figure 6, is associated with the same process.

The 150-dbar surface was chosen to demonstrate subsurface flow features because it is approximately at the dividing depth between PW and AIW over the eastern part of the EGPF. A contour interval of 1 dyn cm was necessary to show the major features, a scaling that admittedly gives results somewhat sensitive to noise and low station density. The geopotential isopleths are surprisingly similar to those at the surface, one important difference being the intensification of the flow westward toward Belgica Dyb as compared with the surface. Otherwise the speeds are generally 3 to 10 times less than at the surface. This is typical of baroclinic shears calculated from historical data. There is little basis for comparison with the measurements from Arlis II [*Aagaard and Coachman*, 1968a], which found relatively small decreases of velocity with depth, because of the presumed large winter-to-summer difference cited by those authors.

Some baroclinic transports have been calculated. For the line along 78°N, a volume flow of $1.2 \times 10^6$ m³/s was computed between the surface and the 500-m level or bottom, whichever was shallower. Assuming that the velocity decreases linearly to near zero at the coast suggests the addition of about $0.8 \times 10^6$ m³/s, summing to a total baroclinic transport of about $2 \times 10^6$ m³/s from the ice edge to land. There are too many uncertainties to estimate an actual transport. The 500-dbar reference level undoubtedly is too shallow, and it is by no means certain that 1000 dbar would be adequately deep. There is the likelihood of a significant barotropic component, according to the results of *Aagaard and Coachman* [1968a].

An illustration of the effects of changing reference level may be had by computing transports for the stations of Atka 1962 along 78°N (Figure 9). Their stations 27, 26, and 38 extend just west of the eastern end of our line on 78°N to 5°E longitude [*Gladfelter*, 1964]. When 500 dbar was used as the reference pressure, the southward transport was $0.5 \times 10^6$ m³/s. When 2500 dbar was the reference pressure, not only did the velocities in the upper 500 m increase, which would lead to more than doubling of the transport in the upper 500 m, but also the increased thickness of the transporting water column resulted in a transport of $3.4 \times 10^6$ m³/s.

It is interesting that at this latitude the Atka 1962 results show that part of the southward flowing water is east of any manifestation of PW and thus, nominally, is not part of the EGC. Evidently, association of the edge of the EGC with the 0°C isotherm is somewhat arbitrary.
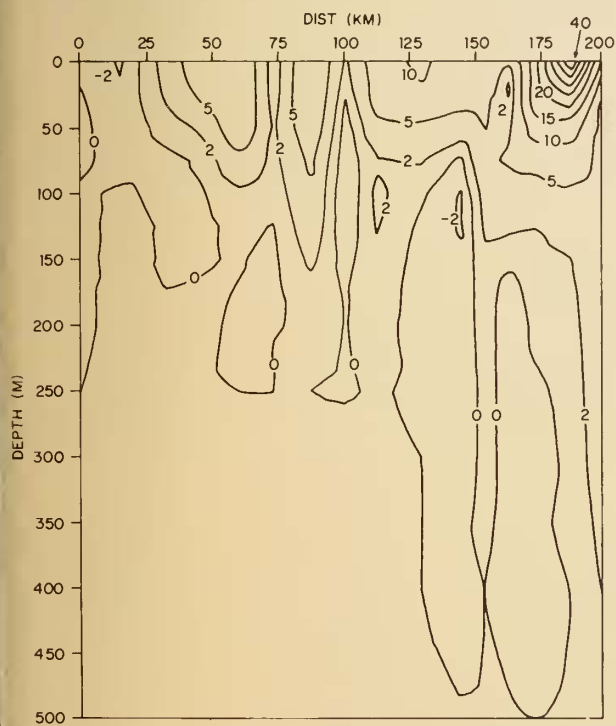


Fig. 14. A section showing baroclinic north-south components of speed along 78°10′N in transect 5, Figure 5. Speeds are in centimeters per second (multiply by 0.01 to obtain meters per second), positive toward the south. This is a transect with only a moderate speed in the frontal jet. The narrowness of the frontal jet is notable. The variability in speeds is interesting, although perhaps not yet interpretable.
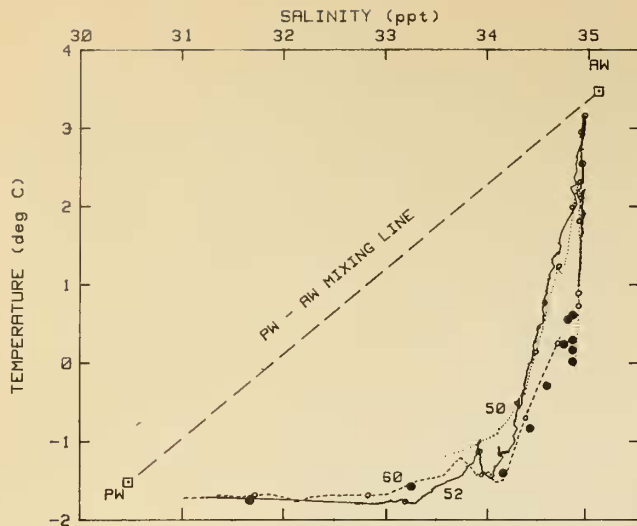
Fig. 15. Temperature-salinity correlations for selected stations along the length of transect 4. Symbols on the curves are every 40 m, beginning at 40 m. The water labeled PW approximates the composition of the locally available PW of lowest salinity. The composition of the AW source is estimated for this season by a small extrapolation from the warmest and most saline water observed during the cruise. The deep knee in the curves near −1.2°C and salinity 34.1 cannot have been formed by mixing of PW and AW. Arctic Ocean water at 83 30.8′N, 13°41′W is indicated by solid circles.

## TEMPERATURE-SALINITY RELATIONS

The temperature-salinity diagram of Figure 15 illustrates the water masses present at three stations spanning the more southerly cross section along 78°N (Figure 4). The symbols on the curves mark 40-m depth intervals, beginning at 40 m and extending to beyond 480 m in two of the three stations. The narrow peak of warm AW or AIW is connected by a deep dip or knee in the curve with a sequence of waters within the PW definition. These ultimately connect with water having a salinity of about 30.5 and a temperature near −1.5°C that may be regarded as the effective low-salinity source for mixing. This is the water labeled PW on the curve. Similar T-S relations were shown by nearly all the stations in the cruise. The exceptions

are those stations that did not have PW in the upper layers, principally the first nine stations. Figure 15 exemplifies the fact that a maximum in salinity in each lowering is closely associated with the deepest temperature maximum or is at a slightly deeper depth, as may be seen most easily in Figure 16. Considering all the stations in the cruise that exhibit a knee, the temperatures at the knee are coldest at the most westerly stations. Only one station was so far west that no warming of the bottom water above 0°C occurred.

It is evident from the deep knee in the curves between the AIW beneath and the PW above that the waters between are not the product of simple mixing between these two waters: they are too cold. The primary mechanism for formation of the knee is undoubtedly the advection of AIW from the east under the outflowing upper layers of Arctic Ocean water. At least some of the Arctic Ocean water is like that of the more westerly stations of 1981, e.g., station 50. This may be seen in Figure 15, where the solid circles trace the properties of station 268 of Arlis II [Tripp and Kusunoki, 1967] at 83°30.8′N, 13°41′W, about 400 km NNW of Fram Strait in December 1964. The temperature maximum is rather broad and is located between 290 and 440 m depth. The knee is at 118 m depth. Obviously, the Arctic Ocean water has not been simply underrun by AIW with properties like those of stations 50 and 52; there has been a modification, and there is not enough information available to determine how this modification takes place.

One modifying process likely to go on at the upper interface of the warm RAC with PW is double diffusion. We have followed the methods of earlier authors [e.g., Horne, 1978] in computing the heat loss from the warm layer, recognizing that the equations used are an extrapolation from laboratory scale that has not been well verified on oceanic scales. The rate of exchange of heat and salt across the "diffusive" interface separating the two water masses was calculated. For the heat flux rate $H$, Horne's equation reduces to

$$H = 250.2 \, \Delta T^{4/3} \, R_\rho^{-2} \qquad \text{W m}^{-2}$$

where the temperature difference $\Delta T$ was taken to be 4°C (from 2.5°C to −1.5°C). The density ratio $R_\rho = \beta \, \Delta S / \alpha \, \Delta T$ was computed to be 2.86, using a salinity difference $\Delta S$ of 1.0
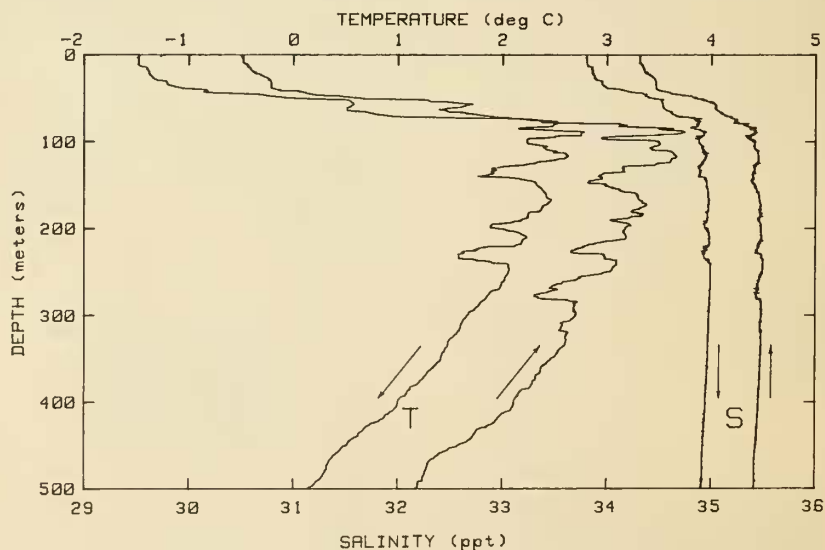


Fig. 16. Temperature and salinity profiles, station 95. Both down and up traverses are shown. This station shows the most notable fine structure in the cruise. The total elapsed time for both profiles is 28 min. A new fine structure element has appeared in the up-going temperature profile during a period of about 17 min.

over the depth interval from 75 to 175 m. These are average conditions for the warmer parts of the RAC. A density ratio of 2.86 implies a relatively stable interface [Turner, 1965], leading to a small salt flux rate but a moderate heat flux rate. A heat flux rate of 194.2 W m$^{-2}$ ($4.69 \times 10^{-5}$°C m s$^{-1}$) was calculated. The salt flux rate was approximately $4.8 \times 10^{-7}$ kg m$^{-2}$ s$^{-1}$ ($4.7 \times 10^{-7}$‰ m s$^{-1}$).

In comparison, Carmack and Aagaard [1973] computed a flux rate of $3.6 \times 10^{-3}$ cal cm$^{-2}$ s$^{-1}$ (151 W m$^{-2}$, $3.64 \times 10^{-5}$°C m s$^{-1}$) between the AIW and overlying PW in the central Greenland Sea in winter in a water column with lower stability than ours but a compensating smaller temperature gradient. As a result their number is similar to ours. Carmack and Aagaard regarded this flux as large enough to produce Greenland Sea Bottom Water from the AW.

To reduce the heat flux rate calculated above to more easily understandable terms, a hypothetical model is proposed that has only a limited relation to reality. Suppose that a 100-m-thick block of 2.5°C AIW flows under PW, which maintains its lower surface at constant depth and at a constant temperature of $-1.5$°C by whatever process maintains the temperature structure of the PW (more about this assumption later). Heat then diffuses upward from the AIW at the rate calculated for the finally developed thermocline above. This is a conservative calculation because the temperature gradients during the entire process would be larger than the final value for which the above heat rate was calculated. The heat loss from the AIW layer during the production of the linear temperature ramp would then be $8.4 \times 10^8$ J m$^{-2}$. In this calculation we give no insight into the detailed mechanisms that cause the resulting ramp to form. This process would require 50 days at the computed rate of heat transfer. The AIW could have been in contact with the PW for this rather long period of time if the original underflow occurred perhaps 150-km upstream and the AIW moved southward to the present latitude, with its mean velocity of about 0.03 m s$^{-1}$. This would put the original underflow at about 81°N, which is reasonable, indicating that to some fraction of an order of magnitude double diffusion can be an important element in the heat transfer.

An objection to this calculation is the assumption that the PW layer maintains its temperature structure as well as a strong salinity and density gradient; it does not appear to be warmed by the rising heat, and there appears to be no rapid mechanism to bring the heat into contact with melting ice. However, the PW travels southward much more rapidly than the AIW, as was shown in the last section, and the PW modifications would eventually accumulate many kilometers downstream. This cannot be demonstrated conclusively in the present data because of the coupling of seasonal effects with the spatially changing properties as the waters move downstream.

## Fine Structure

Along the EGPF, as at most water mass boundaries, notable temperature inversions having thicknesses within the fine-structure range are formed by the interleaving of dissimilar water masses. The temperature profile from station 95 (Figure 16) is an example of one of the more striking cases. This and other stations along the EGPF demonstrate lenses of alternately cool and warm water with peak-to-peak excursions of 0.5°C to 1.0°C embedded in the profile and most strikingly evident in the AIW at depths just below the temperature maximum. The stations having notable structure in the AIW are shown in Figure 2 as solid circles. They are generally present along the EGPF associated with the warm core of the RAC.

The temperature and salinity cross sections show that most of the fine structure is located in the AIW between 75 and 300 m depth, being shallower toward the seaward edge of the front. The transect along 77°N (Figure 8), for example, illustrates that near the eastern edge of the front the fine structure is centered between 100 and 200 m depth and slowly deepens westward, along nearly constant salinity surfaces, which are also nearly isopycnals. These sections also indicate that the fine-structure elements are not long in the cross-frontal direction but are either lenses or north-south oriented filaments of anomalously warmer or cooler water embedded in the surrounding water. In the ensuing discussion the term lenses will be used for convenience, with a recognition that what is seen as a lens in an east-west section may be elongated north-south.

There also is fine structure in the positive-going temperature ramp of the main thermocline, which also includes much of the PW. This structure appears to have causes not greatly different from those that cause fine structure in the AIW.

The sources of the contrasting interleaving waters in the warm core probably ultimately are parcels of AIW from east of the EGPF that have descended from near or at the surface along the isopycnal surfaces of the sloping front, as seen in Figures 4–8. Various combinations of slight dilution of AW by PW and surficial cooling by the atmosphere are possible in this source region, producing waters of different temperatures but equal densities. The fine structure observed in the main thermocline, both in the PW and the AIW, also has connecting isopycnal surfaces to waters of varying properties near or at the surface.

In Figure 17 is shown an expanded T-S plot of the fine-structure region of station 95. The depth zone from 70 to 400 m is plotted with asterisks indicating depth increments of approximately 11 m, beginning at 70 m. The salinities have been
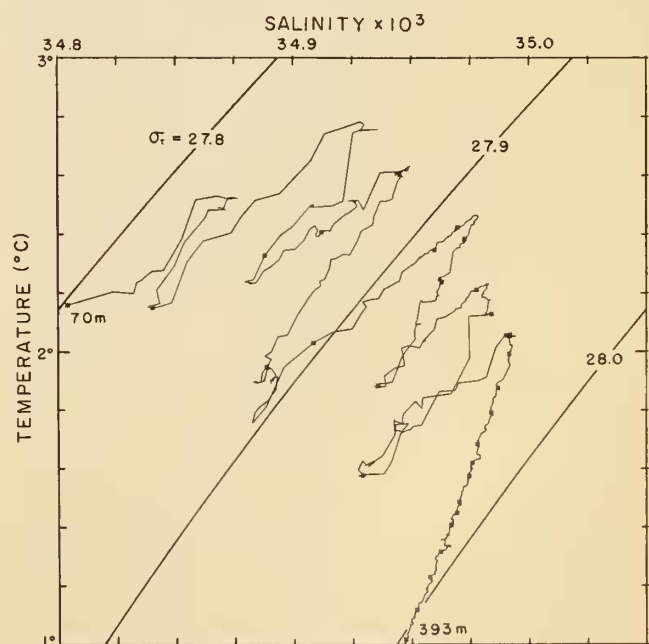


Fig. 17. Expanded temperature-salinity diagram for station 95. Only the portion between 70 and 390 m, which contains most of the major fine structure, is plotted. The asterisks along the curve indicate depth increments of about 11 m, beginning at 70 m. The salinity has been despiked amd smoothed with a five-point running mean. It is remarkable that the density increases relatively monotonically at this high resolution in a region so disturbed. The density inversions near the T-S extrema are predictable (see text).

despiked and smoothed with a five-point running mean. The alternating warm and cold lenses are seen to increase in sigma-t nearly monotonically throughout the depth range as a result of compensating temperature and salinity excursions. The unstable loops near several of the temperature-salinity extrema are similar to those described as being due to double-diffusive mixing by *Posmentier and Houghton* [1978]. However, these may be due to imperfect despiking.

The fine-structure lenses can be expected to tend to dissipate by double-diffusive processes. Each lens has on one surface a salt-finger interface and on the other a diffusive interface. Using the laboratory-derived data of *Turner* [1965, 1967], as formulated by *Huppert* [1971] for salt-finger interfaces and by *Horne* [1978] for diffusive interfaces, vertical heat and salt flux rates were calculated from the fine-structure profiles of six stations in the frontal area. These six stations were representative of the more energetic interleaving situations. A total of 21 salt-finger and 21 diffusive interfaces were present in these profiles. The mean density ratio associated with each type of interface was 1.09 and 1.59, respectively, indicating that both types of interface were inherently unstable and were candidate boundaries for double-diffusive convective mixing. The mean heat fluxes across the salt-finger and diffusive interfaces were 38.5 $W/m^2$ and 58.2 $W/m^2$, respectively. These numbers may be divided by $4.138 \times 10^6$ to obtain units of degrees Centigrade per meter per second. The mean salt flux rates were very small.

Common practice in computing dissipation times for fine-structure elements is to assume that the heat flux is constant and to compute the time until no temperature signal remains. This must yield a time that is too short because the rate actually must decrease as the temperature difference decreases. A closer estimate may be obtained by computing the time as though the temperature difference could be replaced by the temperature gradient and by applying a diffusion equation. This is likely to be a reasonable assumption over large distances compared to the laboratory scale from which the heat flux equations are derived. Under these conditions, heat is exchanged very slowly as the temperature difference becomes small, and complete dissipation is never attained.

In the salt-finger case, where the rate is proportional to the temperature difference, the Fickian diffusion law then applies. In the diffusive case the rate is proportional to the 10/3 power of the temperature difference, and a modified diffusion equation applies. The diffusive interface is found to degenerate very slowly, after an initial rapid change, and the salt-finger interface causes most of the degeneration. The mechanism by which a fine-structure element dissipates, then, is one in which the temperature maximum drives heat downward to fill the trough between itself and the next maximum beneath with a little help from the diffusive interface beneath driving heat upward.

It was found possible to solve simple cases of the 10/3-power law numerically. The simple case of a temperature ramp in salt-finger diffusion degenerating by redistribution of heat within the original space can be solved easily by means of the classical diffusion equation applied to a thermally insulated rod [Pipes, 1958, p. 496]. However, the case of heat diffusing upward by the 10/3-power law in part of the fine-structure element and downward by a first-power law in the remainder of the element, although solvable, is unjustifiably complicated. After some experimentation it was concluded that a reasonable approximation to the more complex process might be had by modeling the fine structure as shown in Figure 18, where two temperature peaks of the same amplitude, one
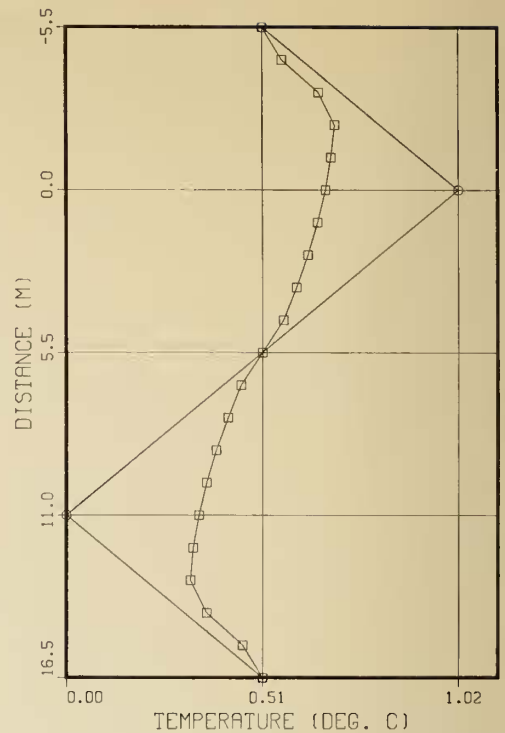


Fig. 18. A practical modeling of the average fine-structure element described in the text. Heat diffuses downward by a first-power diffusion law to convert the initial idealized peak into the illustrated result, 63% dissipation in 3 days.

above the other, are assumed to degenerate only by Fickian diffusion acting in one direction, from $-1/4\lambda$ to $+3/4\lambda$, where $\lambda$ is the distance between the peaks.

For the mean salt-finger case, $\Delta T = 1.02°C$, $\lambda = 22$ m, and the diffusion constant is 0.99 gcal $cm^{-1}$ $s^{-1}$ $°C^{-1}$. By the method just discussed, degeneration occurred by 70% in 4 days and by 90% in 9.5 days. By the Pipes solution for an 11-m-long temperature ramp the respective times are 5.7 and 12 days. The assumption of constant rate, redistributing heat in the $1/2\lambda$ space between peak and trough, gives 7 days for complete dissipation. While we believe the first method to be philosophically more pleasing, the present limited state of knowledge about diffusion rates at oceanic-length scales makes the relatively small differences between the methods seem unimportant.

Such short lifetimes would result in the disappearance of the fine structure if it were not continually regenerated. Our observations indicate that the fine structure continues to exist all along the front for time periods at least as long as the 6-week sampling period of the cruise. In another sense, if the fine structure advected from a northern source, it would have to traverse several hundred kilometers at the drift rate of the AIW, of the order of 2–3 km/d. Thus there must be a continual resupply of contrasting water types from the east.

On several casts a fine-structure lens present during lowering was absent during hoisting, usually some 20–30 min later. The reverse situation was also observed. An example of the latter can be seen in Figure 16, where a large intrusion centered near 275 m is present in the upward traverse of station 95 but is totally absent in the downward traverse. It is apparent that the ship drifted into the path of this lens in the short interval between lowering and hoisting. Station 96 (Figure 8), taken 2.5 hours later and 7 km farther westward, shows a similar situation, except that here the intrusive features ob-
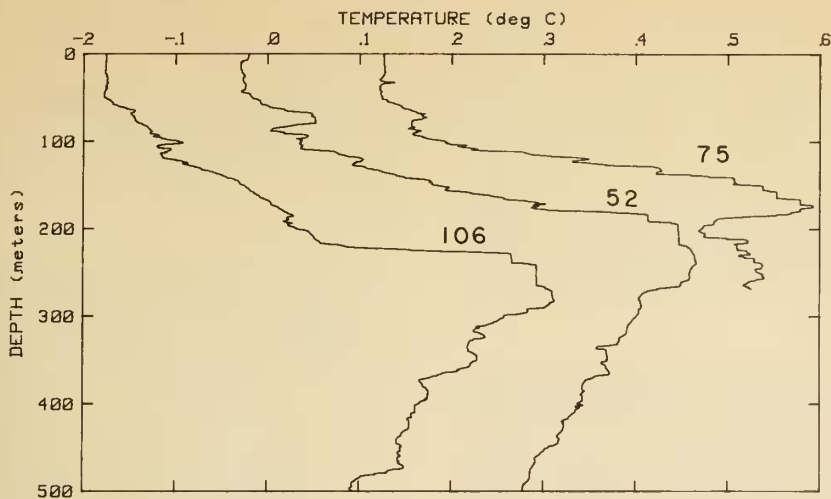
Fig. 19.   Temperature profiles, stations 52, 75, and 106. The temperature graduations are correct for station 106; the other two are offset to the right 1.5°C and 3.0°C, respectively. These are the only profiles showing notable staircase fine structure.

served on the lowering are absent on the upward CTD traverse. This appearance of disappearance of a notable fine-structure element is not common; it occurs in roughly 3% of elements with peak-to-peak amplitudes greater than 0.3°C, even in regions where the vertical velocity shear was several tenths of a meter per second. Assuming that on the average the ship drifted 0.4 m/s, relative to the fine structure, for 1020 s (17 min) between up and down traverses, the lengths of the lenses of water in the direction of the current shear must be at least $0.4 \times 1020 = 408$ m. If it is assumed that all the elements are of equal length, that the probability of starting an observation anywhere along the length is the same, and that disappearances are equal in number to appearances, then observing the disappearance of a terminus in 1.5% of the cases suggests that the minimum length estimate should be multiplied by 1/0.015, yielding an average length estimate of 27 km. Inspection of Figure 8 indicates that the larger elements (those not obscured by the contouring process) have a comparable length in the east-west direction.

Marked staircase temperature structure was present in the pycnocline of three profiles. Stations 52, 75, and 106 demonstrate these diffusive interfaces near the end of the large temperature ramp connecting cold PW with warm AIW (Figure 19). Station 75 exhibits three diffusive interfaces separated by nearly isothermal layers; two such interfaces are observed in the temperature profiles of stations 52 and 106. Many staircase structures in the temperature-step range of 0.02–0.1°C are to be found in other stations. These smaller steps are similar to those observed in the positive-gradient portions of temperature profiles from the central Arctic basin [Neshyba et al., 1971] and from the Weddell Sea [Middleton and Foster, 1980]. Structures such as these are likely to have been formed from double-diffusive convective processes [Turner, 1973].

SUMMARY

A number of closely spaced salinity and temperature measurements were made crossing the EGPF in a number of places between 76°N and 79°N in October-November of 1981. The measurements revealed a rich fine structure in a warm core of water consisting mostly of AIW east of and under the PW. Comparison with historical data shows this core, termed the Return Atlantic Current, to be substantially warmer in

autumn 1981 than in earlier summers. In summer the temperature front was vertical and even reversing slope near the surface, whereas the salinity front was similar in slope winter and summer and about the same slope as the autumn temperature front: 4–14 m/km.

The Return Atlantic Current had a core of AW on 78°N, but at more southerly positions was AIW, slightly cooler and more dilute than AW. Between it and the PW above was a layer of cooled but only slightly diluted water showing evidence of a double-diffusive interchange with the PW. This layer also exists widely in historical water columns in the area that have supernatant PW.

A near-surface frontal jet, with velocities greater than 0.80 m/s in some places, was concentrated within a narrow strip with thicknesses less than 150 m. The highest velocities were associated with the highest station densities, suggesting that high velocities might be found all along the front if the station density were high enough. This also explains the failure to find such high velocities in historical, low-resolution data. Except for the jet itself, baroclinic surface velocities were comparable in magnitude to earlier Lagrangian measurements. The dynamic topographies at depth did not support the maintenance of speed with depth found by Aagaard and Coachman [1968b] in winter by direct measurement from the ice island Arlis II.

A sharp turning of the baroclinic circulation westward toward the coast of Greenland near 77°N has some historical support and is believed to be due to an influence of the onshelf depression called the Belgica Dyb. The turning is seen to be stronger at the 150-dbar level than at the surface. The propagation of AIW westward in this same location may be seen in the property cross sections.

When AIW underlies PW, a knee is formed in the temperature-salinity diagram as a result of the presence of a cold, saline water, colder than could be formed by linear mixing of PW and AW. Advection from the Arctic Ocean, formation in winter, or loss of heat by double diffusion are possible explanations for its formation.

Pronounced temperature fine structure was present in the frontal area, most notably in the AIW underneath the temperature maximum of the Return Atlantic Current. This is a depth zone with a small vertical density gradient; nevertheless the density increased monotonically with depth, with minor

exceptions. Fine structure also was present above the temperature maximum in the main thermocline and extended past the 0 C boundary into PW. Three profiles with relatively large staircase fine structure were found in this depth zone. The steep rise of isopycnals into the near-surface zone to the east suggests that the source of warm and cold components of the fine structure, both above and below the temperature maximum, is in this zone. Some such continual source is required because otherwise the rates of double diffusion are great enough to have caused the effective dissipation of the fine structure in 4–12 days.

## REFERENCES

Aagaard, K., and L. K. Coachman, The East Greenland Current north of Denmark Strait, 1, *Arctic, 21*(3), 181–200, 1968a.

Aagaard, K., and L. K. Coachman, The East Greenland Current north of Denmark Strait, 2, *Arctic, 21*(3), 267–290, 1968b.

Aagaard, K., and P. Greisman, Toward new mass and heat budgets for the Arctic Ocean, *J. Geophys. Res., 80*(27), 3821–3827, 1975.

Bourke, R. H., R. G. Paquette, and J. L. Newton, Fine structure and double diffusion in the East Greenland Polar Front, *Eos Trans. AGU, 64*(52), 1059, 1983.

Carmack, E., and K. Aagaard, On the deep water of the Greenland Sea, *Deep Sea Res., 20*, 687–715, 1973.

Codispoti, L. A., Some results of an oceanographic survey in the northern Greenland Sea, summer 1964, *Tech. Rep. 202*, 49 pp., U. S. Nav. Oceanogr. Office, Washington, D. C., 1968.

Dietrich, G., Atlas of the hydrography of the northern North Atlantic, 140 pp., Int. Counc. Explor. Sea, Copenhagen, 1969.

Gladfelter, W. H., Oceanography of the Greenland Sea, USS *Atka* (AGB-3) survey summer 1962, *Informal Rep. 0-64-63*, 154 pp., U. S. Nav. Oceanogr. Office, Washington, D. C., 1964.

Horne, E. P. W., Interleaving at the subsurface front in the slope water off Nova Scotia, *J. Geophys. Res., 83*(C7), 3659–3671, 1978.

Huppert, H. E., On the stability of a series of double-diffusive layers, *Deep Sea Res., 18*, 1005–1021, 1971.

Jakhelln, A., Oceanographic investigations in East Greenland waters in the summers of 1930–1932, *Skr. Svalbard Ishavet, 67*, 79, 1936.

Kiilerich, A. B., On the hydrography of the Greenland Sea, *Medd. Groenl., 144*(2), 63, 1945.

Middleton, J. H., and T. D. Foster, Fine structure measurements in a temperature-compensated halocline, *J. Geophys. Res., 85*(C2), 1107–1122, 1980.

Neshyba, S., V. T. Neal, and W. Denner, Temperature and conductivity measurements under ice island T-3, *J. Geophys. Res., 76*, 8107–8120, 1971.

Newton, J. L., and L. E. Piper, Oceanographic data from the northwest Greenland Sea: Arctic east 1979 survey of USCGC *Westwind*, *Rep. SAI-202-81-003-LJ*, Sci. Appl., Inc., San Diego, Calif., 1981.

Perdue, W. F., Oceanographic investigation of the East Greenland Polar Front, Master's thesis, Nav. Postgrad. School, Monterey, Calif., 1982.

Pipes, L. A., *Applied Mathematics for Engineers and Physicists*, 723 pp., McGraw-Hill, New York, 1958.

Posmentier, E. S., and R. W. Houghton, Fine structure instabilities induced by double diffusion in the shelf/slope water front, *J. Geophys. Res., 83*(C10), 5135–5138, 1978.

Scientific Committee for Oceanographic Research, The Arctic Ocean heat budget, Report from Working Group 58, *Rep. 52*, Geophys. Inst., Univ. Bergen, Norway, 1979.

Smith, D. C., J. H. Morison, J. A. Johannessen, and N. Untersteiner, Topographic generation of an eddy at the edge of the East Greenland Current, *J. Geophys. Res., 89* (C5), 8205–8208, 1984.

Swift, J. H., and K. Aagaard, Seasonal transitions and water mass formation in the Iceland and Greenland seas, *Deep Sea Res., 28A*(10), 1107–1129, 1981.

Tripp, R. B., and K. Kusunoki, Physical, chemical, and current data from Arlis II: Eastern Arctic Ocean, Greenland Sea, and Denmark Strait area, February 1964–May 1965, *Tech. Rep. 185*, vols. 1 and 2, *Ref. M67-29*, Dep. Oceanogr., Univ. Wash., Seattle, 1967.

Turner, J. S., The coupled turbulent transports of salt and heat across a sharp density interface, *Int. J. Heat Mass Transfer, 8*, 759–767, 1965.

Turner, J. S., Salt fingers across a density interface, *Deep Sea Res., 14*, 599–611, 1967.

Turner, J. S., *Buoyancy Effects in Fluids*, 367 pp., Cambridge University Press, New York, 1973.

Vinje, T. E., Sea ice conditions in the European sector of the marginal seas of the Arctic, 1966–75, *Arbok Nor. Polarinst. 1975*, 163–174, 1977a.

Vinje, T. E., Some observations from Nimbus-6 data collecting platforms in polar seas, paper presented at the Joint IAGA/IAMAP Assembly, Seattle, WA, 22 Aug–3 Sept, 1977b.

Vinje, T. E., Sea ice conditions and drift of Nimbus-6 buoys in 1977, *Arbok Nor. Polarinst. 1975*, 283–292, 1978.

Vinje, T. E., Sea ice conditions and drift of Nimbus-6 buoys in 1978, *Arbok Nor. Polarinst., 1976*, 57–66, 1979.

Wadhams, P., and V. A. Squire, An ice-water vortex at the edge of the East Greenland Current, *J. Geophys. Res., 88*(C5), 2770–2780, 1983.

Wadhams, P., A. E. Gill, and P. F. Linden, Transects by submarine of the East Greenland Polar Front, *Deep Sea Res., 26*(12A), 1311–1328, 1979.

R. H. Bourke and R. G. Paquette, Naval Postgraduate School, Monterey, CA 93943.

J. F. Newton, Science Applications, Inc., La Jolla, CA 92037.

W. F. Perdue, Naval Eastern Oceanographic Center, Naval Air Station, Norfolk, VA 23511.

INITIAL DISTRIBUTION LIST

19. Project Manager
    Anti-Submarine Warfare Systems Project
    Office (PM4)
    Department of the Navy
    Washington, District of Columbia 20360                              1

20. Commanding Officer
    Naval Underwater Systems Center                                     1
    Newport, Rhode Island 02840

21. Commander
    Naval Air Systems Command                                          1
    Headquarters
    Department of the Navy
    Washington, District of Columbia 20361

22. Commander
    Naval Oceanographic Office
    Attn:  Library Code 3330
    Washington, District of Columbia 20373                             1

23. Director
    Advanced Research Project Agency                                   1
    1400 Wilson Boulevard
    Arlington, Virginia 22209

24. Commander SECOND Fleet
    Fleet Post Office                                                  1
    New York, New York 09501

25. Commander THIRD Fleet
    Fleet Post Office                                                  1
    San Francisco, California 96601

26. Commander
    Naval Surface Weapons Center
    White Oak
    Attn:  Mr. M.M. Kleinerman                                         1
           Library                                                     1
    Silver Springs, Maryland 20910

27. Officer-in-Charge
    New London Laboratory                                             1
    Naval Underwater Systems Center
    New London, Connecticut 06320

28. Commander
    Submarine Development Group TWO                                    1
    Box 70
    Naval Submarine Base
    New London
    Groton, Connecticut 06340

29.  Commander
     Naval Weapons Center
     Attn:  Library                                                    1
     China Lake, California 93555

30.  Commander
     Naval Electronics Laboratory Center
     Attn:  Library                                                    1
     271 Catalina Boulevard
     San Diego, California 92152

31.  Director                                                          1
     Naval Research Laboratory
     Attn:  Technical Information Division
     Washington, District of Columbia 20375

32.  Director                                                          1
     Ordnance Research Laboratory
     Pennsylvania State University
     State College, Pennsylvania 16801

33.  Commander Submarine Force                                         1
     U.S. Atlantic Fleet
     Norfolk, Virginia 23511

34.  Commander Submarine Force
     U.S. Pacific Fleet                                                1
     Attn:  N-21
     FPO San Francisco, CA 96860

35.  Commander                                                         1
     Naval Air Development Center
     Warminster, Pennsylvania 18974

36.  Commander                                                         1
     Naval Ship Research and Development Center
     Bethesda, Maryland 20084

37.  Commandant                                                        1
     U.S. Coast Guard Headquarters
     400 Seventh Street, S.W.
     Washington, DC 20590

38.  Commander                                                         1
     Pacific Area, U.S. Coast Guard
     630 Sansome Street
     San Francisco, California 94126

39.  Commander                                                         1
     Atlantic Area, U.S. Coast Guard
     159E, Navy Yard Annex
     Washington, District of Columbia 20590

| | | |
|---|---|---|
| 40. | Commanding Officer<br>U.S. Coast Guard Oceanographic Unit<br>Building 159E, Navy Yard Annex<br>Washington, District of Columbia 20590 | 1 |
| 41. | Scientific Liaison Office<br>Office of Naval Research<br>Scripps Institute of Oceanography<br>La Jolla, California 92037 | 1 |
| 42. | SIO Library<br>Scripps Institute of Oceanography<br>P.O. Box 2367<br>La Jolla, California 92037 | 1 |

43. University of Washington
    Attn:   Dept. of Oceanography Library          1
            Dr. L.K. Coachman                      1
            Dr. K. Aagaard                         1
            Dr. S. Martin                          1
    Seattle, Washington 98105

44. Library, School of Oceanography              1
    Oregon State University
    Corvallis, Oregon 97331

45. CRREL
    U.S. Army Corps of Engineers
    Attn:   Library                               1
    Hanover, New Hampshire 03755

46. Commanding Officer                            1
    Fleet Numerical Oceanography Center
    Monterey, California 93940

47. Commanding Officer                            1
    Naval Environmental Prediction Research Facility
    Monterey, California 93940

48. Defense Technical Information Center          2
    Cameron Station
    Alexandria, Virginia 22314

49. Commander                                     1
    Naval Oceanography Command
    NSTL Station
    Bay St. Louis, Mississippi 39529

50. Commanding Officer
    Naval Ocean Research and Development Activity
    Attn:   Technical Director                    1
            Dr. J.P. Welsh,                       1
    NSTL Station
    Bay St. Louis, Mississippi 39529

51. Commanding Officer                                                      1
    Naval Polar Oceanography Center, Suitland
    Washington, District of Columbia 20373

52. Director                                                                1
    Naval Oceanography Division
    Naval Observatory
    34th and Massachussetts Ave. NW
    Washington, District of Columbia 20390

53. Commanding Officer
    Naval Oceanographic Command                                             1
    NSTL Station
    Bay St. Louis, Mississippi 39522

54. Scott Polar Research Institute
    University of Cambridge
    Attn:  Library                                                          1
           Sea Ice Group                                                    1
    Cambridge, England
    CB2 1ER

55. Chairman                                                                1
    Department of Oceanography
    U.S. Naval Academy
    Annapolis, Maryland 21402

56. Dr. James Morison                                                       1
    Polar Science Center
    4059 Roosevelt Way, NE
    Seattle, Washington 98105

57. Dr. Kenneth Hunkins                                                     1
    Lamont-Doherty Geological Observatory
    Palisades, New York 10964

58. Dr. David Paskowsky, Chief                                              1
    Oceanography Branch
    U.S. Department of the Coast Guard
    Research and Development Center
    Avery Point, Connecticut 06340

59. Science Applications, Inc.
    Attn:  Dr. Robin Muench                                                 1
    13400B Northrup Way
    Suite 36
    Bellevue, Washington 98005

60. Institute of Polar Studies
    Attn:  Library                                                          1
    103 Mendenhall
    125 South Oval Mall
    Columbus, Ohio 43201

61. Institute of Marine Science
    University of Alaska
    Attn: Library                                          1
    Fairbanks, Alaska 99701

62. Department of Oceanography
    University of British Columbia
    Attn: Library                                          1
    Vancouver, B.C. Canada
    V6T 1W5

63. Geophysical Institute
    University of Alaska
    Attn: Dr. H.J. Niebauer                                1
    Fairbanks, Alaska 99701

64. Bedford Institute of Oceanography
    Attn: Library                                          1
    P.O. Box 1006
    Dartmouth, Nova Scotia
    Canada
    B2Y 4A2

65. Carol Pease                                            1
    Pacific Marine Environmental Lab/NOAA
    7600 Sand Point Way N.E.
    Seattle, Washington 98115

66. Department of Oceanography                             1
    Dalhousie University
    Halifax, Nova Scotia
    Canada
    B3H 4J1

67. Mr. Richard Armstrong                                  2
    MIZEX Data Manager
    National Snow and Ice Data Center
    Cooperative Institute for Research
     in Environmental Sciences
    Boulder, Colorado 80309